Indian Journal of Pure & Applied Physics
Vol. 52, August 2014, pp. 507-519

Comparative DFT study on reactivity, acidity and vibrational spectra of halogen substituted phenylacetic acids

Ambrish K Srivastava[1], Vikas Baboo[2], B Narayana[3], B K Sarojini[4] & Neeraj Misra[1]*

[1]Department of Physics, University of Lucknow, Lucknow 226 007, India

[2]Department of Chemistry, University of Lucknow, Lucknow 226 007, India

[3]Department of Studies in Chemistry, Mangalore University, Mangalagangotri 574 199, Karnataka, India

[4]Department of Chemistry, PA College of Engineering, Mangalore 574 153, Karnataka, India

*E-mail: neerajmisra11@gmail.com

Received 4 May 2013; revised 17 December 2013; accepted 20 March 2014

A detailed first principle study on the three halogenated phenylacetic acid i.e. 2-(2-halophenyl)acetic acid where –halo=fluoro/chloro/bromo has been carried out. The calculated structural properties show close resemblance with the crystallographic data. The reactivity of molecules using various descriptors –local such as fukui functions, local softness and electrophilicity as well as –global i.e. electronegativity, hardness, HOMO-LUMO gap etc. along with acidity of the same are calculated and discussed. The vibrational spectra of chloro-and bromo-substituted molecules are calculated and compared with those obtained with experimental FTIR method while that of fluoro-substituted is predicted theoretically.

Keywords: Phenylacetic acid, Halogen substitution, Reactivity, Acidity, DFT, FTIR

1 Introduction

Phenylacetic acid (PA) is one of the most popular biomolecules. It works well as a precursor for synthesizing many drugs and chemicals in which a particularly remarkable one is Penicillin G also named as benzylpenicillin, is a popular member of the group of very old and well known antibiotics-Penicillin. PA is fed in to small amounts to the medium to avoid toxic effect during biosynthesis[1] of Penicillin G. It has also been found to be a potent therapeutic agent for the treatment of human cancer[2] since human beings are capable to detoxify PA by conjugation with glutamine. Anti-fungal, anti-microbial, anti-inflammatory and analgesic actions of PA have been well studied and reported[3-5]. Recently, a theoretical study on PA has also been performed[6].

Several derivatives of PA show promising biological activities as well[7-9]. The halogen derivatives of PA have been found to have anti-proliferative and anti-tumor properties against various types of cancer. They are found to be more active for estrogen receptor positive cells[10]. The PA derivative of progesterone, when substituted with halogen, shows high potent antagonistic activity for progesterone receptor[11]. Thus, the incorporation of halogen in PA imparts special features and increases its bioactivity in one way or other. This attracted us to perform a comparative study of halogen substituted PA.

The detailed study of 2-(2-Halophenyl) acetic acid [$C_8H_7XO_2$] (X: F/Cl/Br) performed at B3LYP level using 6-311++G** as a basis set, is reported in the present paper. We have used DFT herein to explore various electronic properties, relative reactivity and acidity of these halogenated PA. Vibrational spectra are also calculated for all the three substitution.

2 Experimental Details

The compounds 2-(2-chlorophenyl)acetic acid and 2-(2-bromophenyl)acetic acid were purchased from Sigma Aldrich with a purity of 98%. These were used as such without further purification for spectroscopic processing. The IR spectra were recorded by using Shimadzu-Model Prestige 21 spectrometer in the region 400-4000 cm^{-1} with samples in KBr pellet.

3 Theoretical Methodology and Computational Details

All the studies have been carried out with Gaussian 03 W suite of programs[12] using density functional theory (DFT). The molecular properties were calculated at B3LYP level in which Becke's three parameter exchange functional[13] was combined with the Lee, Yang and Parr correlation functional[14]. The

B3LYP functional has become universal choice to study the biomolecules due to the fact that it offers a good compromise between desired accuracy and affordable cost[15]. The geometry of molecules was optimized without any constraint in the molecular potential energy surface (PES) to give minimum energy conformer using 6-311++G** basis set. The relevant structures and plots were created by Gauss-View[16], a popular GUI of Gaussian.

The electronic properties and associated parameters were calculated with optimized structures. In order to calculate various parameters, two different strategies were adopted viz. electron-vertical method (EVM) and orbital-vertical method (OVM). EVM gives ionization potential (I) or electron affinity (A) from the difference between energies of neutral molecule and its cation or anion, respectively. In OVM, on the other hand, negative energy eigen-value of the highest occupied molecular orbital (HOMO) and that of lowest unoccupied (LUMO) gives directly I and A, respectively. Other chemical descriptors are calculated[17-20] as below:

Electro-negativity index, $\chi \approx (I + A)/2$
Chemical hardness, $\eta \approx (I - A)/2$
Global softness, $S = 1/2\eta$
Electrophilicity, $\omega = \chi^2/2\eta$

Fukui function ($f_k^{\pm}$), local softness ($s_k^{\pm}$) and local electrophilicity ($\omega_k^{\pm}$) give an indication of relative reactivity of atomic sites in the molecule which are calculated[18-21] as:

$f_k^{+} = [q(N+1) - q(N)]$, for nucleophilic attack

$f_k^{-} = [q(N) - q(N-1)]$, for electrophilic attack

$s_k^{\pm} = S\, f_k^{\pm}$ and $\omega_k^{\pm} = \omega\, f_k^{\pm}$

where q(N) is the charge on k^{th} atom for neutral molecule while q(N+1) and q(N−1) are the same for its anionic and cationic species, respectively. The above parameters were computed using Hirshfeld scheme of charges. This scheme yields an optimal partitioning of the electron density and seems to work efficiently due to its less basis set dependency[22].

In many biological systems, proton-transfer reactions take place to provide communication between the exo and intra cellular media. The acidity constant, pK_a, of a compound is an important property and is fundamental in understanding of many chemical and biochemical processes. The geometries of the neutral and deprotonated species are fully optimized at the B3LYP/6–311++G** level of theory. Solvent effects (calculated in water) are taken into account by means of the polarizable continuum model (PCM). Free energy change in aqueous medium ($\Delta G^\circ_{aq.}$) is calculated as:

$$\Delta G^\circ_{aq.} = G^\circ_{aq.}(A^-) + G^\circ_{aq.}(H^+) - G^\circ_{aq.}(AH)$$

The given scheme explains the inter-relationship between the thermodynamic parameters of gas and solution phases.

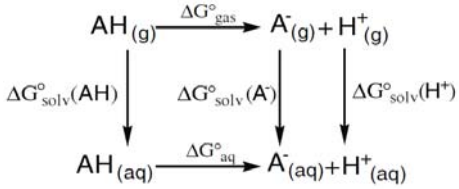

The pK_a is calculated accordingly as:

$$pK_a = \frac{\Delta G^\circ_{aq}}{2.303RT}$$

Vibrational analysis was carried out at the same level of theory for the optimized structures i.e. there were no imaginary frequency found for any halogenated PA. The computed frequencies were scaled with a factor[23] of 0.96 to compensate for basis set deficiencies to some extent. Normal modes were assigned on the basis of calculated infrared intensities and compared with experimental FTIR data. The potential energy distribution (PED) was calculated with the help of VEDA program[24].

4 Results and Discussion

4.1 Structural properties

The optimized geometries for halogenated PA at B3LYP/6-311++G** level are shown in Fig. 1. Various geometrical parameters as calculated with optimized structures are organized in Table 1, appendix Tables A1 and A2 with experimental values[25,26]. The dihedral angle O16-C15-C12-C2 of –COOH group with the phenyl ring is found to be 11.2° and −12.4° for chlorine and bromine, respectively while for fluorine corresponding dihedral O15-C14-C11-C1 is considerably small, 5.09°. These are, in turn, very smaller than corresponding value[6] for PA. This shows that the substitution of halogen in

PA tends to deform the structure due to steric effects. The internal bond angle at the carbon atom attached with halogen is 123.3° for fluorine which is consistently greater than 122.0° for chlorine and 122.4° for bromine. This exceeds the normally adopted internal bond angle for phenyl ring. An opposite trend is found for the bond angle at carbon atom attached with $–CH_2COOH$ group, 116.8° for fluorine, 117.2° for chlorine and 117.1° for bromine that is smaller than corresponding value for PA. The calculated values agree well with experimental bond lengths and bond angles.

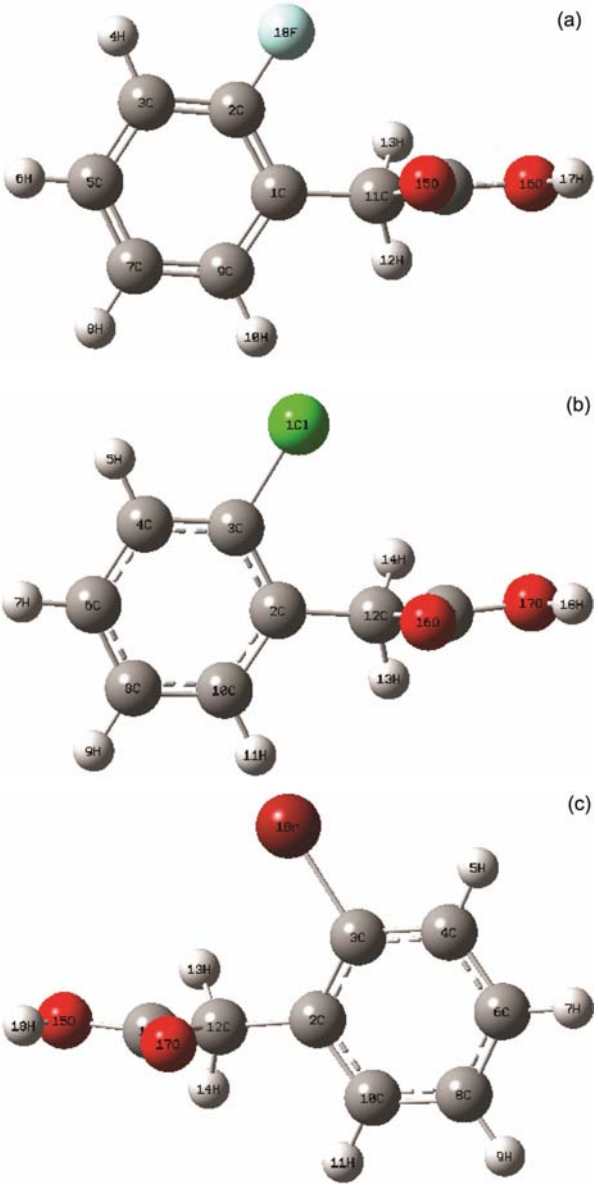

Fig. 1 — Optimized geometry for (a) fluoroPA at B3LYP/6-311++G**, (b) chloroPA at B3LYP/6-311++G** and (c) bromoPA at B3LYP/6-311++G**

4.2 Electronic properties

The electronic properties of molecule are related to the geometry of an isolated molecule but they provide a lot of information about macroscopic properties of molecular system in condensed phases. The total energy for neutral molecule E_N with its cation E_C and anion E_A and other parameters along with various chemical descriptors calculated are given in Table 2(a) and (b). There are remarkable differences in the results obtained from EVM and OVM. The reason behind this is the validity of Koopmans' theorem, on which OVM rests, is limited to unrelaxed orbitals. It considers neither orbital relaxation effects nor electron correlation effectively. These effects cause to shift HOMO eigen-values up and LUMO eigen-values down from negative ionization potentials and negative electron affinities, respectively[27-30]. The ionization potentials calculated by EVM are larger than those by OVM while electron affinities are smaller. These results agree well with above facts. It is interesting to note that the differences become smaller with heavier halogens characterizing properties of its orbitals.

4.2.1 Global reactivity descriptors

Chemical descriptors provide a great insight into chemical reactivity and hence biological activity of the molecule. The chemical bond properties and charge densities in a molecule can be well analyzed by its dipole moment. The dipole moments calculated for halogenated PA, as given in are a bit higher[6] than that for PA which is 1.5276 D. This indicates that the substitution of halogen Table 2(a), in PA tends to make it relatively more polarized. The total energy E_N for neutral molecules listed in Table 2(a) shows that fluorine closely mimics hydrogen as a second smallest substituent. The difference in energies[6] for fluoroPA and PA is near about 100 hartree.

The chemical hardness gives a quantitative measurement of stability of a molecule while electro-negativity tells the strength to attract electrons in a chemical bond. The calculation clearly shows the decrease in stability with the substitution of heavier halogen. In the bonding, where partial charge transfer takes place, electrophilicity decides the energy lowering due to maximum electron flow from donor to acceptor. The calculated values for all the three halo derivatives of PA are listed in Table 2(b).

Table 1 — Bond-lengths of three haloPA calculated at B3LYP/6-311++G** level. Corresponding experimental values are also listed

Bond length (A°)	fluoroPA Calc.	Bond length (A°)	chloroPA Calc.	chloroPA Expt	Bond length .(A°)	bromoPA Calc.	bromoPA Expt.
C1-C2	1.3919	Cl1-C3	1.7632	1.742	Br1-C3	1.9241	1.901
C1-C9	1.3972	C2-C3	1.3990	1.384	C2-C3	1.3994	1.380
C1-C11	1.5049	C2-C10	1.3987	1.384	C2-C10	1.3997	1.383
C2-C3	1.3843	C2-C12	1.5057	1.508	C2-C12	1.5062	1.502
C2-F18	1.3591	C3-C4	1.3911	1.374	C3-C4	1.3917	1.383
C3-H4	1.0828	C4-H5	1.0824	0.930	C4-H5	1.0822	0.930
C3-C5	1.3935	C4-C6	1.3919	1.370	C4-C6	1.3922	1.361
C5-H6	1.0837	C6-H7	1.0838	0.930	C6-H7	1.0839	0.930
C5-C7	1.3935	C6-C8	1.3926	1.376	C6-C8	1.3923	1.378
C7-H8	1.0834	C8-H9	1.0836	0.930	C8-H9	1.0836	0.930
C7-C9	1.3932	C8-C10	1.3913	1.377	C8-C10	1.3909	1.360
C9-H10	1.0849	C10-H11	1.0849	0.930	C10-H11	1.0849	0.930
C11-H12	1.0939	C12-H13	1.0944	0.970	C12-H13	1.0918	0.970
C11-H13	1.0933	C12-H14	1.0922	0.970	C12-H14	1.0946	0.970
C11-C14	1.5200	C12-C15	1.5203	1.492	C12-C16	1.5203	1.491
C14-O15	1.2020	C15-O16	1.2020	1.227	O15-C16	1.3570	1.304
C14-O16	1.3576	C15-O17	1.3572	1.293	O15-H18	0.9691	0.870
O16-H17	0.9691	O17-H18	0.9691	0.820	C16-O17	1.2021	1.218

Calc. – Calculated, Expt. –Experimental

Table 2(a) — Energies, HOMO-LUMO gaps and dipole moments of three haloPA at B3LYP/6-311++G**

Molecule	E_N (a.u.)	E_A (a.u.)	E_C (a.u.)	ε_{HOMO} (a.u.)	ε_{LUMO} (a.u.)	E_{gap} (eV)	M (Debye)
fluoroPA	–559.5374	–559.522	–559.203	–0.259	–0.032	6.176	1.8935
chloroPA	–919.8905	–919.876	–919.561	–0.257	–0.033	6.095	1.9117
bromoPA	–3033.8096	–3033.792	–3033.484	–0.255	–0.034	6.013	1.8668

Table 2(b) — Global descriptors for three halo PAs calculated at B3LYP/6-311++G** level

Global Descriptors	fluoroPA EVM	fluoroPA OVM	chloroPA EVM	chloroPA OVM	bromoPA EVM	bromoPA OVM
I (a.u)	0.3344	0.259	0.3295	0.257	0.3256	0.255
A (a.u)	0.0154	0.032	0.0145	0.033	0.0176	0.034
η (a.u)	0.1595	0.1135	0.1575	0.112	0.1540	0.1105
χ (a.u)	0.1749	0.1455	0.1720	0.1450	0.1717	0.1445
ω (a.u.)	0.0958	0.0933	0.0939	0.0938	0.0957	0.0945
S (a.u)	3.1347	4.4053	3.1746	4.4643	3.2467	4.5249

4.2.2 HOMO-LUMO analyses

The HOMO and LUMO, also known as frontier orbitals, are responsible for reaction or interaction with other chemical species. In fact, all the features discussed above can be restated in terms of HOMO and LUMO. The corresponding energy eigen-values ε_{HOMO} and ε_{LUMO} are calculated in Table 2(a) with their differences known to be as an energy gap E_{gap}. Due to virtue of smaller E_{gap} bromoPA seems to be more chemically reactive than other halogenated PA. The energy gap, being neither too small nor too large, can explain the charge transfer interaction (CTI) within the molecules. The trend for CTI is F < Cl < Br.

The HOMO-LUMO plots for neutral halogenated PA are shown in Fig. 2 in which colour coding scheme is used to represent charge densities. The HOMOs are seen to be localized on phenyl ring and methylene (–CH_2) group excluding carboxylic acid (–COOH) group while LUMOs are contributed by molecules as a whole. The incorporation of halogen

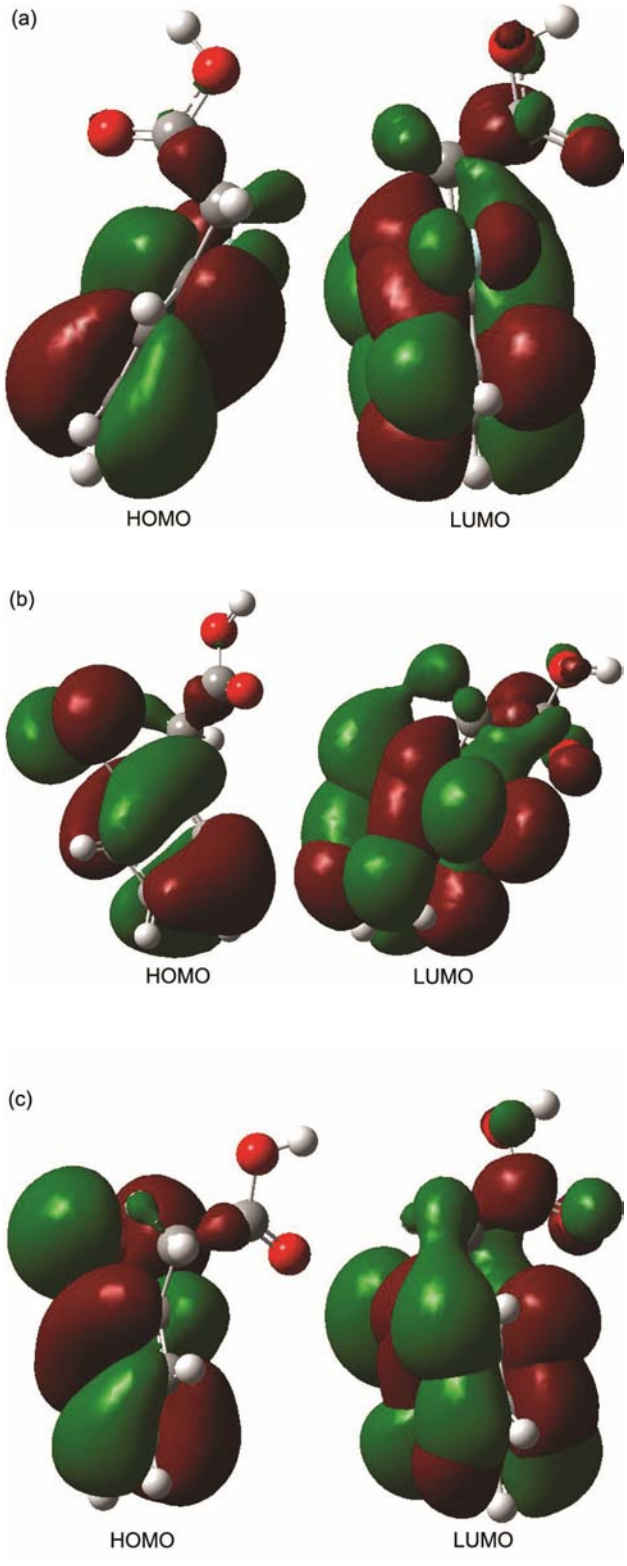

Fig. 2 — Plots for (a) fluoroPA, (b) chloroPA and (c) bromoPA at B3LYP/6-311++G**

alters charge distribution in molecule hence their structural, electronic and vibrational properties.

5 Local Reactivity Descriptors

The exceptional quality of the Fukui functions (FF) using the perturbational approach gives the necessary confidence for the application of the novel methodology in the computation of local descriptors. These descriptors are used to decide relative reactivity of different atoms in the molecule. It has been established that molecules tend to react where the value of descriptors is the largest when attacked by soft reagents and in places where the value is smaller when attacked by hard reagents[31]. Possible negative values for the Fukui indexes have been considered as artifacts coming from the condensation procedure or due to strong structural distortions. The values calculated at B3LYP/6-311++G** level of theory using hirshfeld charges on atoms in molecule are presented in Table 3(a) and (b). The use of descriptors for the site selectivity of the molecule for nucleophilic and electrophilic attacks has been made for halogenated PA. The calculated local FFs, local softness and local electrophilicity index stated that the atomic site C11 of acid and C5 on benzene ring are prone to nucleophilic attack while C7 is the most active site for electrophilic attack in case of fluoroPA. The calculated values indicate that, it might be possible the p-substitution easily takes place in fluoroPA. For chloroPA and for bromoPA nucleophilic substitution favours C8 and C6, respectively while electrophilic attack is most likely to occur on C8. For chloroPA and bromoPA, C15 sites of carbonyl group, are also favourable for the nucleophilic attack. This site is predicted to be the most reactive for nucleophilic attack in all the derivatives of PA.

6 Acidity Calculations

The aqueous–phase acidity of the carbon acid series under study can be explained by the relative stabilities of their anions. The anions are stabilized by a combination of resonance, electromeric and inductive effects[32]. Furthermore, it has been showed that delocalization or resonance stabilization is an important factor responsible for improved acidity. Acidity increases when the delocalization of the negative charge (in the carbanion) increases[33-35].

The pK_a values of PA derivatives at 6–311++G** in aqueous phase are given in Table 4 which were calculated at 298.15°C. The value of ΔG_{aq} (H^+),-271.2

Table 3(a) — Local reactivity descriptors for fluoroPA at B3LYP/6-311++G** level

Atom No.	f_k^+	f_k^-	s_k^+	s_k^-	ω_k^+	ω_k^-
C1	0.0111	0.1791	0.0488	0.7889	0.001	0.0167
C2	0.0156	0.1454	0.0687	0.6406	0.0015	0.0136
C3	0.0756	0.0017	0.333	0.0076	0.0071	0.0002
C5	0.1476	0.1253	0.6501	0.5518	0.0138	0.0117
C7	0.1441	0.2516	0.6346	1.1086	0.0134	0.0235
C9	0.1193	-0.031	0.5255	-0.136	0.0111	-0.003
C11	0.1573	-0.019	0.6928	-0.082	0.0147	-0.002
C14	0.0385	-0.199	0.1695	-0.875	0.0036	-0.019

Table 3(b) — Local reactivity descriptors for chloroPA and bromoPA at B3LYP/6-311++G** level

Atom No.	f_k^+ Cl / Br	f_k^- Cl/Br	s_k^+ Cl/Br	s_k^- Cl/Br	ω_k^+ Cl/Br	ω_k^- Cl/Br
C2	0.010/0.011	0.066/0.059	0.047/0.050	0.298/0.270	0.001/0.001	0.006/0.005
C3	0.014/0.015	0.088/0.0788	0.063/0.068	0.394/0.356	0.001/0.001	0.008/0.007
C4	0.076/0.083	0.087/0.083	0.339/0.376	0.390/0.379	0.007/0.007	0.008/0.007
C6	0.148/0.154	0.122/0.111	0.660/0.698	0.546/0.503	0.013/0.014	0.011/0.010
C8	0.151/0.150	0.170/0.162	0.675/0.681	0.760/0.735	0.014/0.014	0.016/0.015
C10	0.126/0.131	0.080/0.078	0.563/0.596	0.357/0.355	0.011/0.012	0.007/0.007
C12	0.151/0.144	0.064/0.057	0.677/0.654	0.289/0.260	0.014/0.013	0.006/0.005
C15	0.037/0.177	0.015/0.049	0.166/0.803	0.068/0.221	0.003/0.016	0.001/0.004

Table 4 — Aqueous phase solvation free energies of halogenated PA at B3LYP/6-311++G** level

Molecules	G°(A^-) (a.u.)	G°(H^+) (a.u.)	G°(AH) (a.u.)	ΔG° (kcal/mol)	pK_a
FluoroPA	–559.0009	–0.4322	–559.4502	10.7457	7.88
ChloroPA	–919.3649	–0.4322	–919.8038	4.2302	3.10
BromoPA	–3033.2764	–0.4322	–3033.7254	10.5492	7.73

kcal mol^{-1} was used as suggested in the literature[36]. Using calculated values of pK_a, it was found that the chloroPA is more acidic than other halogenated PA because of its quite lower value of pK_a. Thus, the anion majority of chlorine substituted PA is greater than that of bromoPA and fluoroPA. The calculated dipole moment values also favour this trend.

7 Vibrational Analysis

Vibrational studies reveal the dynamical behaviour of a molecular system. Many important aspects can be explored by the same study which may be very significant for the evaluation of properties and utilization of molecules. The halogenated PA has C_1 point group of trivial symmetry and 48 normal modes of vibration. The detailed assignments of vibrational modes along with the calculated IR intensities are presented in Table 5(a), (b) and (c) which are characterized by PED. For comparison, experimental FTIR values are also included, wherever possible, for chloroPA and bromoPA. Due to unavailability of fluoroPA compound, we were unable to present experimental FTIR for fluoroPA. However, this provided us a unique opportunity to analyze vibrational properties of fluoroPA purely theoretically, reported in Table 5(c). The corresponding IR spectra are presented in Fig. 3(a), (b) and (c) for a visual indication.

7.1 Ring vibration

7.1.1 C-H modes

The substituted aromatic structure shows the presence of C–H stretching vibration in the region 3100-3000 cm^{-1}, which is the characteristic region for the identification of C–H stretching vibrational modes[37,38]. In this region, the bands are not affected appreciably by the nature of the substituent. The calculated C–H modes are found between 3080 cm^{-1}

Table 5(a) — Vibrational modes for chloroPA calculated at B3LYP/ 6-311++G** level (experimental FTIR frequencies are also given)

Scaled Freq. (cm^{-1})	IR Int. (au)	FTIR (cm^{-1})	PED mode assignments (coordinate)
3608	76.10		Acetic [100% ν OH (S_1)]
3074	3.67		Ring [79% ν_s CH (S_2)+16% ν_s CH (S_3)]
3063	12.28		Ring[14% ν_{as} CH (S_2)+16% ν_s CH (S_3)+ 61% ν_s CH (S_4)]
3048	7.79		Ring [62% ν_s CH (S_3)+14% ν_{as} CH (S_4)+18% ν_{as} CH (S_5)]
3037	3.78		Ring [21% ν_{as} CH (S_4)+73% ν_s CH (S_5)]
2971	0.88		Acetic [23% ν_{as} CH (S_6)+76% ν_s CH (S_7)]
2929	9.35		Acetic [76% ν_s CH (S_6)+23% ν_s CH (S_7)]
1748	263.95		Acetic [87% ν OC (S_8)]
1571	4.63	1581	Ring [26% ν_s CC (S_9)+13% ν_s CC (S_{12})]
1546	7.01		Ring [30% ν_s CC (S_{11})+18% ν_{as} CC (S_{13})+10% δ_i CCC (S_{27})]
1446	28.00		Ring [21% δ_i HCC (S_{20})+13% δ_o HCC (S_{22})+23% δ_o HCC (S_{23})+12% δ_i CCC (S_{28})]
1415	20.83	1415	Ring [10% ν_{as} CC (S_9)+11% ν_s CC (S_{13})+26 % δ_o HCC (S_{21})+15% δ_o HCC (S_{22})]
1400	20.21		Acetic [55% δ HCH (S_{25})+10% τ_i HCCO (S_{39})+17% τ_o HCCO (S_{40})]
1327	62.97	1344	Acetic [10% ν_{as} OC (S_{14})+13% ν_s CC (S_{16})+11% τ HOC (S_{19})+20% σ HCH (S_{25}) +11% τ_o HCCO (S_{39})+15% τ_i HCCO (S_{40})]
1279	0.36	1294	Ring [15% ν_{as} CC (S_{10})+s13 24% ν_s CC (S_{13})+10% δ_o HCC (S_{24})]
1260	4.77		Ring [11% ν_{as} CC (S_9)+11% ν_s CC (S_{12})+21% δ_i HCC (S_{23})]+Acetic [17% δ HOC (S_{19})]
1242	0.81	1236	Ring [10% ν_s CC (S_9) +10% δ_o HCC (S_{23})]+Acetic [13% τ_i HCCO (S_{40})+30% δ_i HOC (S_{19})]
1176	4.45	1197	Ring [13% ν_{as} CC (S_9)+27% ν_s CC (S_{15})+12% δ_i HCC (S_{20})]
1163	0.50		Ring [11% ν_s CC (S_{13})+52% δ_i HCC (S_{24})]
1137	0.02	1130	Ring [10% ν_{as} CC (S_{11})+12% δ_i HCC (S_{20})+33% δ_o HCC (S_{21})+31% δ_i HCC (S_{22})]
1101	8.81		Ring [24% ν_s CC (S_{10})+12% ν_{as} CC (S_{12})+16% δ_o HCC (S_{21})+10% δ_o HCC (S_{22})]
1091	376.97	1043	Acetic [53% ν_s OC (S_{14})]+Ring [23% δ_o HOC (S_{19})]
1025	10.37		Ring [15% ν_s CC (S_{11})+17% δ_i HCC (S_{20})+10% δ_o HCC (S_{23})+15% δ_o CCC (S_{27}) +13% δ_o CCC (S_{29})]
1011	42.25		Ring [13% ν_s CC (S_{10})+20% ν_s CC (S_{11})+11% ν_s CC (S_{12})+10% ν_{as} ClC (S_{17})+18% δ_i CCC (S_{27})]
954	0.02	950	Ring [33% τ_o HCCC (S_{36})+34% τ_i HCCC (S_{37})+12% τ_o HCCC (S_{38})+11% τ_o CCCC (S_{43})]
921	2.57	925	Ring [20% τ_i HCCC (S_{35})+15% τ_o HCCC (S_{36})+36% τ_i HCCC (S_{38})+10% τ_i CCCC (S_{43})]
904	6.36		Acetic[32% τ_i HCCO (S_{39})+13% τ_i HCCO (S_{40})+24% τ_o OCOC (S_{46})]
850	4.51		Acetic [30% ν_s CC (S_{16})]+Ring [15% τ_o HCCC (S_{35})+14% τ_i HCCC (S_{38})]
840	4.80		Acetic [11% ν_{as} CC (S_{16})]+Ring [11% δ_i CCC (S_{28})+12% τ_o HCCC (S_{35})+11% τ_i HCCC (S_{38})]
812	14.03		Ring [10% δ_o CCC (S_{28})+11% δ_i CCC (S_{32})+14% τ_o HCCC (S_{35})]
730	52.78	754	Ring [14% τ_i HCCC (S_{35})+28% τ_i HCCC (S_{36})+33% τ_i HCCC (S_{36})+14% τ_i HCCC (S_{38})]
701	10.96		Ring [16% τ_o CCCC (S_{41})+10% τ_i CCCC (S_{42}) +13% τ_o CCCC (S_{43})+16% τ_o CCCC (S_{48})]
666	9.44	675	Ring [15% ν_s ClC (S_{17})+14% δ_o CCC (S_{18})+30% δ_i CCC (S_{29})]
633	53.76		Acetic [21% τ_o HOCC (S_{34})+16% τ_o OCOC (S_{46})]
619	55.52	615	Acetic [12% τ OCO (S_{26})+31% τ_i HOCC (S_{34})+12% τ_o OCOC (S_{46})]
570	38.96		Ring [14% δ_i CCC (S_{18})]+Acetic [41% τ OCO (S_{26})]
499	9.96		Acetic [15% τ_i HOCC (S_{34})+10% τ_i OCOC (S_{46})] +Ring [17% τ_o ClCCC (S_{47})+10% τ_o CCCC (S_{48})]
494	16.52		Acetic [31% τ_i HOCC (S_{34})+24% τ_i OCOC (S_{46})]
435	5.94	437	Ring [11% ν_{as} ClC (S_{17}) +19% τ_o CCCC (S_{41})+10% τ_i CCCC (S_{43})+19% τ_o ClCCC (S_{47})]
422	4.87		Ring [33% ν_s ClC (S_{17})+12% δ_i CCC (S_{27})+13% δ_i CCC (S_{31})]
377	4.63		Acetic [18% τ OCC (S_{30})+Ring [20% δ_i CCC (S_{31})+27% δ_o ClCC (S_{33})]
309	1.38		Acetic [13% ν_s CC (S_{15})+30% σ OCC (S_{30})+Ring[20% δ_i CCC (S_{31})]
264	0.74		Acetic [16% δ OCC (S_{30})]+Ring [19% δ_o CCC (S_{31})+12% τ_o CCCC (S_{43})+19% τ_o ClCCC (S_{47})]
245	0.99		Ring [12% δ_i CCC (S_{31})+48% δ_i ClCC (S_{33})]
149	0.58		Ring [41% τ_i CCCC (S_{42})+16% τ_o CCCC (S_{43})+21% τ_o ClCCC (S_{47})]
80	1.70		Ring [32% δ_i CCC (S_{32})+16% τ_o CCCC (S_{42})+28% τ_o CCCC (S_{48})]
40	0.35		Ring [85% τ_i CCCC (S_{45})]
33	0.93		Acetic adj. Ring [80% τ_i OCCC (S_{44})]

Table 5(b) — Vibrational modes for bromoPA calculated at B3LYP/ 6-311++G** level (experimental FTIR frequencies are also given)

Scaled Freq. (cm^{-1})	IR Int. (au)	FTIR (cm^{-1})	PED mode assignments (coordinate)
3608	76.47		Acetic [100% ν OH (S_1)]
3074	3.64		Ring [82% ν_s CH (S_2)+14% ν_s CH (S_3)]
3062	12.23		Ring [12% ν_{as} CH (S_2)+18% ν_s CH (S_3)+62% ν_s CH (S_4)]
3048	8.12		Ring [62% ν_s CH (S_3)+14% ν_{as} CH (S_4)+18% ν_{as} CH (S_5)]
3037	3.75		Ring [21% ν_{as} CH (S_4)+73% ν_s CH (S_5)]
2973	0.81		Acetic [81% ν_s CH (S_6)+19% ν_{as} CH (S_7)]
2928	9.45		Acetic [19% ν_s CH (S_6)+81% ν_s CH (S_7)]
1748	258.61	1712	Acetic [87% ν OC (S_8)]
1567	5.06		Ring [10% ν_{as} CC (S_{10})+31% ν_s CC (S_{12})]
1542	8.18		Ring [24% ν_{as} CC (S_{10})+12% ν_s CC (S_{11})+15% ν_s CC (S_{13})+10% δ_i CCC (S_{27})+12% δ_o CCC (S_{29})]
1442	24.84	1433	Ring [13% ν_s CC (S_{13})+20% δ_i HCC (S_{20})+13% δ_o HCC (S_{22})+21% δ_o HCC (S_{23})]
1411	21.48	1404	Ring [10% δ_i CCC (S_{18})+26% δ_o HCC (S_{21})+16% δ_o HCC (S_{22})]+Acetic [11% τ_i HCCO (S_{40})]
1399	20.38		Acetic[68% δ HCH (S_{25})]
1327	61.09	1342	Acetic [10% ν_{as} OC (S_{14})+14% ν_s CC (S_{16})+11% τ HOC (S_{19})+16% σ HCH (S_{25})+12% τ_o HCCO (S_{39})+13% τ_i HCCO (S_{40})]
1275	0.48	1296	Ring [11% ν_{as} CC (S_9)+11% ν_{as} CC (S_{11})+12% ν_s CC (S_{12})+13% ν_s CC (S_{13})]+Acetic[10% τ_o HCCO (S_{40})]
1259	4.34		Ring [11% ν_s CC (S_{13})+22% δ_i HCC (S_{23})]+Acetic[17% δ HOC (S_{19})]
1243	1.08	1238	Acetic [31% δ HOC (S_{19})]+Ring[10% δ_o HCC (S_{20})+12% δ_o HCC (S_{23})]
1175	6.20		Ring [23% ν_{as} CC (S_9)+26% ν_s CC (S_{13})+13% δ_i HCC (S_{20})]
1162	0.43		Acetic [43% σ HCH (S_{24}) +16% τ_i HCCO (S_{40})]
1138	0.02		Ring [11% δ_i HCC (S_{20})+31% δ_o HCC (S_{21})+32% δ_o HCC (S_{22})]
1096	1.52		Ring [16% ν_s CC (S_{10})+14% ν_{as} CC (S_{12})+17% δ_o HCC (S_{21})+10% δ_o HCC (S_{22})]
1091	373.58		Acetic [53% ν_s OC (S_{14})+22% ρ HOC (S_{19})]
1023	1.41	1020	Ring [12% ν_s CC (S_{10})+35% ν_s CC (S_{11})+10% ν_s CC (S_{12}) +13% δ_i HCC (S_{20})]
994	48.09		Ring [10% ν_s CC (S_{11})+18% δ_i CCC (S_{27})+15% δ_o CCC (S_{28})+26% δ_i CCC (S_{29})]
952	0.02		Ring [26% τ_o HCCC (S_{36})+28% τ_i HCCC (S_{36})+10% τ_o HCCC (S_{38})+19% % τ_i CCCC (S_{42})]
921	2.38	931	Ring [20% τ_o HCCC (S_{35})+17% τ_i HCCC (S_{36})+36% τ_o HCCC (S_{38})]
903	6.64		Acetic [23% τ_o HCCO (S_{39})+24% τ_o HCCO (S_{40})+21% τ_o OCOC (S_{46})]
851	4.99		Acetic [29% ν_s CC (S_{16})]+Ring [15% τ_i HCCC (S_{35})+11% τ_o HCCC (S_{37})+16% τ_o HCCC (S_{38})]
839	3.20		Acetic [12% ν_s CC (S_{16})]+Ring [13% δ_o CCC (S_{28})+12% τ_o HCCC (S_{35})+12% τ_i HCCC (S_{38})]
811	12.59		Ring [13% δ_i CCC (S_{28})+10% δ_o CCC (S_{32})+13% τ_o HCCC (S_{35})]
728	49.67	729	Ring [13% τ_i HCCC (S_{35})+29% τ_i HCCC (S_{36})+33% τ_i HCCC (S_{37})+14% τ_i HCCC (S_{38})]
698	9.85	673	Ring [13% τ_i CCCC (S_{42})+16% τ_i CCCC (S_{43})+16% τ_o CCCC (S_{48})]
648	6.99		Ring [14% ν_{as} BrC (S_{17})+18% δ_o CCC (S_{29})]
633	64.54		Acetic[26% τ_i HOCC (S_{34})+18% τ_o OCOC (S_{46})]
618	48.39		Acetic[13% δ OCO (S_{26})+29% τ_i HOCC (S_{34})+10% τ_o OCOC (S_{46})]
568	39.99		Acetic[40% δ OCO (S_{26})]
495	18.39		Acetic[35% τ_o HOCC (S_{34})+28% τ_o OCOC (S_{46})]
490	4.40		Ring [15% τ_i CCCC (S_{42})+13% τ_o BrCCC (S_{47})+12% τ_o CCCC (S_{48})]
429	4.16		Ring [10% τ_i HCCC (S_{35})+29% τ_i CCCC (S_{41})+10% τ_o CCCC (S_{43})+21% τ_o BrCCC (S_{47})+11% τ_o CCCC (S_{48})]
381	0.89		Ring [11% ν_s BrC (S_{17})+50% δ_i CCC (S_{31})]+Acetic [12% τ_i HCCO (S_{39})]
355	6.93		Ring [13% ν_s CC (S_{15})+12% ν_s BrC (S_{17})]+Acetic [39% δ OCC (S_{30})]
268	0.99		Ring [30% ν_{as} BrC (S_{17})+11% δ_i CCC (S_{18})] +Acetic [21% δ OCC (S_{30})]
255	0.92		Ring [11% ν_{as} BrC (S_{17})+14% δ_i CCC (S_{32})+18% τ_i CCCC (S_{41})+13% τ_o BrCCC (S_{47})]
210	0.59		Ring [63% δ_i BrCC (S_{33})]
135	1.00		Ring [11% δ_i CCC (S_{32})+33% τ_i CCCC (S_{43})+35% τ_o BrCCC (S_{47})]
79	1.49		Ring [32% δ_o CCC (S_{32})+29% τ_o CCCC (S_{48})]
37	0.73		Acetic adj. Ring [30% τ_o OCCC (S_{44})]+Ring [55% τ_o CCCC (S_{45})]
32	0.52		Acetic adj. Ring [46% τ_o OCCC (S_{44})]+Ring [33% τ_o CCCC (S_{45})]

Note-PED less than 10% are not included in assignments

Abbreviation-Freq. = Frequency, Int. = Intensity, adj. = adjacent to

Symbols-ν = Stretching, ν_s = Symmetric Stretching, ν_{as} = Asymmetric Stretching, δ = Scissoring, σ = Rocking, τ = Twisting, ρ = Wagging, δ_i = in plane bend, δ_o = out of plane bend, τ_i = in plane torsion, τ_o = out of plane torsion

Table 5(c) — Vibrational modes for fluoroPA calculated at B3LYP/ 6-311++G**

Scaled Freq. (cm^{-1})	IR Int. (au)	PED mode assignments (coordinate)
3609	75.59	Acetic [100% ν OH (S_1)]
3073	2.62	Ring [75% ν_s CH (S_2) + 18% ν_s CH (S_3)]
3064	13.09	Ring [18% ν_{as} CH (S_2) +15% ν_s CH (S_3) +60% ν_s CH (S_4)]
3049	7.08	Ring [62% ν_s CH (S_3) +16% ν_{as} CH (S_4) + 15% ν_{as} CH (S_5)]
3037	4.04	Ring [18% ν_{as} CH (S_4) + 78% ν_s CH (S_5)]
2965	0.98	Acetic [42% ν_{as} CH (S_6) + 58% ν_s CH (S_7)]
2930	10.04	Acetic [58% ν_s CH (S_6) +42% ν_s CH (S_7)]
1749	270.95	Acetic [86% ν CO (S_8)]
1590	7.13	Ring [15% ν_s CC (S_9) + 11% ν_{as} CC (S_{10}) + 25% ν_s CC (S_{13})]
1560	18.51	Ring [18% ν_{as} CC (S_{10}) + 29% ν_s CC (S_{11}) +11% δ_i CCC (S_{18}) + 13% δ_i CCC(S_{29})]
1464	60.59	Ring [10% ν_s CC (S_{10}) + 19% δi HCC (S_{20}) + 19% δ_o HCC (S_{23})]
1427	20.48	Ring [25% δ_i HCC (S_{21}) + 25% δ_o HCC (S_{22})]
1397	18.99	Acetic [63% δ HCH (S_{25}) + 11% τ_i HCCO (S_{39}) + 15% τ_o HCCO (S_{40})]
1327	64.35	Acetic [10% ν_s OC (S_{10}) + 14% ν_{as} CC (S_{17}) + 11% δ HOC (S_{19}) + 12% τ_i HCCO (S_{39}) + 14% τ_o HCCO (S_{40}) + 17% ρ HCH (S_{25})]
1291	0.61	Ring [17% ν_{as} CC (S_9) + 18% ν_s CC (S_{10}) + 17% ν_{as} CC (S_{12}) + 16% ν_s CC (S_{13})]
1261	6.97	Acetic [15% δ HOC (S_{19})] + Ring [29% δ_i HCC (S_{23})]
1243	0.07	Acetic [33% δ HOC (S_{19}) + 15% σ HCCO (S_{40})]
1200	54.65	Ring [14% ν_{as} CC (S_9) + 14% ν_{as} CC (S_{11}) + 28% ν_s FC (S_{16}) + 10% δ_i HCC (S_{20})]
1168	18.24	Ring [10% δ_i CCC (S_{18})] + Acetic [50% δ HCC (S_{24})]
1151	26.76	Ring [11% ν_{as} CC (S_{13}) + 10% ν_{as} FC (S_{16}) + 12% δ_o HCC (S_{22}) + 13% δ_i HCC (S_{23})]
1130	0.15	Ring [11% ν_{as} CC (S_{12}) + 17% δ_i HCC (S_{20}) + 29% δ_i HCC (S_{21}) + 27% δ_i HCC (S_{22})]
1090	372.43	Acetic [54% ν_s OC (S_{14}) + 23% ρ HOC (S_{19})]
1076	25.16	Ring [14% ν_{as} CC (S_{13})]
1012	4.36	Ring [16% ν_s CC (S_{11}) + 38% ν_s CC (S_{12}) + 14% ν_s CC (S_{13}) + 15% δ_i HCC (S_{20})]
942	0.01	Ring [26% τ_i HCCC (S_{36}) + 29% τ_o HCCC (S_{37}) + 10% τ_i HCCC (S_{38}) + 19% τ_o CCCC (S_{43})]
915	3.54	Ring [16% τ_o HCCC (S_{35}) + 19% τ_i HCCC (S_{36}) + 35% τ_o HCCC (S_{38})]
904	8.35	Ring [10% δ_i CCC (S_{29})] + Acetic [24% τ_o HCCO (S_{39}) + 12% τ_i HCCO (S_{40}) + 20% τ_o OCOC (S_{46})]
850	2.80	Acetic [31% ν_s CC (S_{17})] + Ring [14% τ_o HCCC (S_{35})]
846	12.83	Ring [12% ν_s CC (S_{15}) + 17% δ_i CCC (S_{28})]
816	14.59	Acetic [16% ν_s CC(S_{17})] + Ring [22% τ_i HCCC (S_{35}) + 11% τ_o HCCC (S_{38})]
760	9.68	Ring [11% ν_s CC (S_9) + 14% ν_s CC (S_{10}) + 18% ν_s FC (S_{16}) + 18% δ_i CCC (S_{29})]
735	67.62	Ring [28% τ_i HCCC (S_{36}) + 36% τ_i HCCC (S_{37}) + 16% τ_i HCCC (S_{38}) + 10% τ_o FCCC (S_{47})]
701	0.34	Ring [11% τ_i HCCC (S_{35}) + 13% τ_o CCCC (S_{41}) + 11% τ_o CCCC (S_{43}) + 11% τ_o CCCC (S_{48})]
627	50.19	Acetic [14% τ OCO (S_{26}) + 24% τ_o HOCC (S_{34}) + 16% τ_o OCOC (S_{46})]
622	57.03	Acetic [11% δ OCO (S_{26}) + 31% τ_o HOCC (S_{34}) + 16% τ_o OCOC (S_{46})]
575	29.37	Acetic [33% OCO (S_{26})] + Ring [16% δ_o CCC (S_{27})]
526	24.31	Ring [11% ν_{as} FC (S_{16}) +16% δ_o CCC (S_{27}) +10% δ_i CCC (S_{28}) + 12% δ_i CCC (S_{29})]
519	3.18	Ring [12% τ_o HCCC (S_{36}) + 27% τ_o CCCC (S_{43}) + 28% τ_o FCCC (S_{47})]
493	21.12	Acetic [33% τ_i HOCC (S_{34}) + 26% τ_i OCOC (S_{46})]
445	6.38	Ring [11% δ_o FCC (S_{32}) + 21% τ_o CCCC (S_{42}) + 10% τ_o FCCC (S_{47}) + 12% τ_o CCCC (S_{48})]
429	6.41	Acetic [11% δ OCC(S_{30})] + Ring [38% δ_i FCC (S_{32})]
285	0.51	Acetic [21% OCC (S_{30})] + Ring [14% δ_o CCC (S_{33}) + 19% τ_i CCCC (S_{42}) +21% τ_o FCCC (S_{47})]
261	2.89	Ring [45% δ_i CCC (S_{31}) + 16% δ_i FCC (S_{32})]
182	0.38	Ring [13% δ_o CCC (S_{33}) + 44% τ_i CCCC(S_{41}) + 15% τ_o CCCC (S_{43})]
82	2.23	Ring [34% δ_o CCC (S_{33}) + 36% τ_i CCCC (S_{48})]
36	0.45	Ring [85% τ_i CCCC (S_{45})]
32	0.63	Acetic adj. Ring [73% τ_i OCCC (S_{44})]

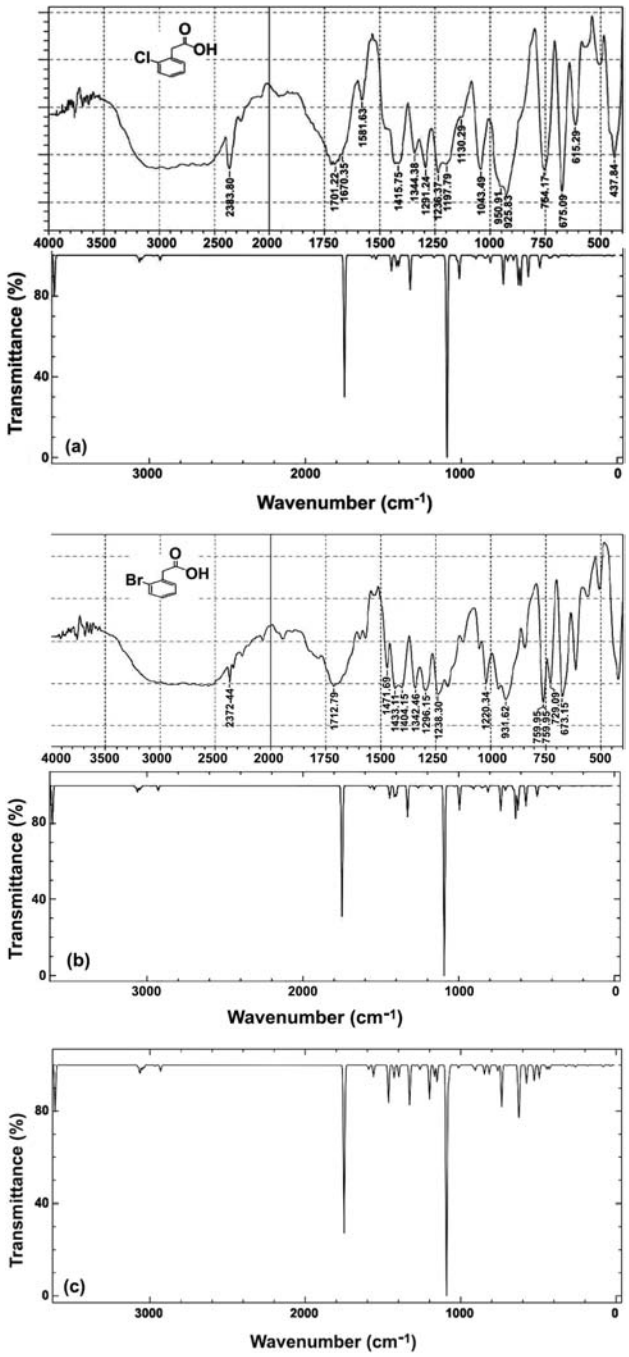

Fig. 3 — Experimental FTIR (up) and simulated IR spectra for (a) chloroPA, (b) bromoPA and (c) simulated IR spectra for fluoroPA at B3LYP/6-311++G**

and 3030 cm^{-1} same for all the three substitutions. These modes are purely stretching having PED greater than 90%. Most of the C–H stretching modes are found to be weak due to charge transfer from hydrogen to carbon atom. Other C–H modes coming from bending (in-plane and out of plane) and torsional vibrations of ring are found in the region below 1500 cm^{-1} having medium to weak intensities.

7.1.2 C-C modes

The C-C ring stretching vibrations[39] are expected within the region 1650-1200 cm^{-1}. Most of these ring modes are altered by the substitution to aromatic ring. Calculated frequencies for C–C and C=C stretching modes at B3LYP/6-311++G** are 1590, 1560, 1464, 1291, 1200 cm^{-1} for fluoroPA while 1571, 1546, 1415, 1260, 1176 cm^{-1} for chloroPA and 1567, 1542, 1442, 1275, 1175 cm^{-1} for bromoPA. Substitution of heavier halogen tends to shift the bands towards lower frequency region. Some other C–C modes associated with bending, torsion, puckering, breathing vibrations of ring are also found in lower frequency region as well as overlapping with other modes. Most of C–C modes are comparatively stronger than C–H modes.

7.1.3 C-X modes

The vibrations corresponding to bonding between the ring and halogen (X) group are significant due to possibility of mixing of vibrations on lowering of the molecular symmetry and the presence of heavy atoms on the periphery of molecule. Mooney[40] assigned vibrations of the C-X group (X= Cl, Br, I) in the frequency range of 1129-480 cm^{-1} while C-F stretching modes are observed to have frequencies above this region[41]. The calculated frequencies of C-F stretching at 1200 and 1151 cm^{-1}, those of C-Cl at 1011, 666 cm^{-1} and C-Br at 633 cm^{-1} agree well with literature values. Other C-X modes associated with bending and torsions are seen in even lower frequency region.

7.2 Acetic group vibration

7.2.1 –COOH group vibration

The vibrational bands of the terminal carboxylic group contain the C–O, C=O and O–H vibrational modes. C=O stretching appears strongly in the region 1870-1540 cm^{-1} while for the O-H, the observed IR frequency region[38] is usually at the interval 3600-3200 cm^{-1}. The modes calculated for O-H at B3LYP level, 3608 cm^{-1} have strong intensity for all the three molecules. The C=O stretching at 1748 cm^{-1} has the strongest intensity. Other pure C=O modes are calculated at 1327 and 1090 cm^{-1}. In plane, out of plane bending and torsion based C=O and C-O modes are calculated to lie in lower frequency range.

7.2.2 –CH_2 group vibration

The C–H stretching modes of the methylene group are at lower frequencies than those of the aromatic C–H ring stretching. The CH_2 anti-symmetric stretching vibrations are generally observed in the region 3000-2900 cm^{-1}, while the CH_2 symmetric stretch[42] will appear between 2900 and 2800 cm^{-1}. The calculated CH_2 anti-symmetric stretching are found at 2965 cm^{-1} for fluoroPA while 2971 cm^{-1} and 2973 cm^{-1} for chloroPA and bromoPA, respectively while symmetric stretching at a little lower frequency. CH_2 bending starts below 1400 cm^{-1} as per B3LYP calculations. It is also found that in mid frequency region CH_2 modes couple with –COOH group vibration as well as with ring vibrations.

8 Conclusions

We have performed the DFT based calculations on halogen substituted phenylacetic acids at B3LYP/6-311++G**. On the basis of our calculations, we can conclude that:

(i) The substitution of heavier halogen tends to affect structural parameters of phenyl acetic acid due to steric effects. This, in turn, cause to make the substituted molecules relatively more polarized as their dipole moments are larger than PA at the same level of theory.

(ii) The substitution of halogen tends to increase the reactivity of molecules. BromoPA is found to be more reactive than other halogenated PA due to its small energy gap between HOMO and LUMO. The lesser chemical hardness value of bromoPA also supports this fact.

(iii) The fluorine closely mimics hydrogen. The maximal Fukui-function values indicate that p-substitution may easily take place in fluoroPA. The carbon site of carboxylic group is prone to nucleophilic substitution in halogenated PA.

(iv) The acidity calculations indicate that the chloroPA is more acidic than other halogenated PA having smaller pk_a value of 3.10. Furthermore, the dipole moment of chloroPA is large as compared to those of fluoroPA and bromoPA.

(v) The vibrational properties are not affected remarkably with the different halogen substitution. However the properties of substituted molecules are quite different as compared[6] to PA.

The calculated values agree well with experimental values. Any discrepancy herein may be due to limitation of calculation on single molecules in gas phase. In condensed phases, the intermolecular interaction i.e. hydrogen bonding, Van der Waal bonding and impurities cause to affect structural as well as vibrational properties. In experimental FTIR, solvent effects greatly influence the vibrational peaks.

Acknowledgement

The authors acknowledge University Grant Commission (UGC) and Council of Scientific and Industrial Research (CSIR), India for the financial support. The author AKS is grateful to CSIR for providing a junior research fellowship.

References

1 Hillenga D J, Versantvoort H J M, Molen S, Driessen A J M & Konings W N, *Appl Environ Microbiol,* 61 (1995) 2589.
2 Neish W J P, *Cell Mol Life Sci,* 27(1971) 860.
3 Hwang B K, Lim S W, Kim B S, Lee J Y & Moon S S, *Appl Environ Microbiol,* 67 (2001) 3739.
4 Kim Y, Cho J Y, Kuk J H, Moon J H, Cho J, Kim Y C & Park K H, *Curr Microbiol,* 48 (2004) 312.
5 Amir M & Shikha K, *Eur J Med Chem,* 39 (2004) 535.
6 Badawi H M &. Förner W, *Spectrochim Acta A*, 78 (2011) 1162.
7 Briquet M V, Decallonne J R, Leblus R G & Wiaux A L, *Biochimica et Biophysica Acta,* 149 (1967) 387.
8 Paronikyan G M & Akopyan L G, *Genetika (Moscow),* 9 (1973) 78.
9 Kuzuna S, Matsumoto N, Morimoto S, Ishii H & Kawai K, *Kenkyushoho,* 34 (1975) 467.
10 Johnson D E, Ochieng J & Evans S L, *Anti-Cancer Drugs,* 7 (1996) 288.
11 Cabeza M, Bratoeff E, Gómez G, Heuze I, Rojas A, Ochoa P, Palomino M A & Revilla C, *J Ster Biochem Mol Biol,* 111 (2008) 232.
12 Frisch M J *et al*., Gaussian 03 Revision B.03, Gaussian Inc. Pittsburgh PA, 2003.
13 Becke. A D, *J Chem Phys,* 98 (1993) 5648.
14 Lee C, Yang W & Parr R G, *Phys Rev B,* 37 (1988) 785.
15 Foresman J B & Frisch A, Exploring Chemistry with Electronic Structure Methods (2nd ed), Gaussian Inc., Pittsburgh PA, 1996.
16 Dennington R, Keith T & Millam J, GaussView Version 3, Semichem Inc KS, 2003.
17 Kohn W, Becke A D & Parr R G, *J Phys Chem*, 100 (1996) 12974.
18 Parr R G & Pearson R G, *J Am Chem Soc,* 105 (1983) 7512.
19 Parr R G, Szentpaly L V & Liu S, *J Am Chem Soc,* 121 (1999) 1922.
20 Chattaraj P K, Lee H &. Parr R G, *J Am Chem Soc,* 113 (1991) 1855.
21 Chattaraj P K & Giri S, *J Phys Chem A*, 111 (2007) 11116.
22 Proft F D, Alsenoy C V, Peeters A, Langenaeker W & Geerlings P, *J Comp Chem,* 23 (2002) 1198.

23 Alecu I M, Zheng J, Zhao Y & Truhlar D G, *J Chem Theory Comput,* 6 (2010) 2872.
24 Jamroz M H, Vibrational Energy Distribution Analysis, VEDA 4, Warsaw, 2004.
25 Kant R, Gupta V K, Kapoor K & Narayana B, *Acta Cryst E,* 68 (2012) o1940.
26 Kant R, Kapoor K & Narayana B, *Acta Cryst E,* 68 (2012) o1704.
27 Allen M J & Tozer D J, *Mol Phys,* 100 (2002) 433.
28 Tozer D J, *J Chem Phys,* 119 (2003) 12697.
29 Tozer D J & Proft F D, *J Phys Chem A,* 109 (2005) 8923.
30 Zhan C G, Nichols J A & Dixon D A, *J Phys Chem A,* 107 (2003) 4184.
31 Ayers P W &. Parr R G, *J Am Chem Soc,* 122 (2000) 2010.
32 Bordwell F G, Bares J E, Bartmess J E, McCollum G J, Puy M V D, Vanier N R & Matthews W S, *J Org Chem,* 42 (1977) 321.
33 Bordwell F G & McCollum G J, *J Org Chem,* 41 (1976) 2391.
34 Hiberty P C & Byrman C P, *J Am Chem Soc,* 117 (1995) 9875.
35 Wiberg K B, Ochterski J & Streitwieser A, *J Am Chem Soc,* 118 (1996) 8291.
36 Sefcık J & Goddard III W A, *Geochimica et Cosmochimica Acta,* 65 (2001) 4435.
37 Rastogi V K, Palafox M A, Tanwar R P & Mittal L, *Spectrochim Acta A,* 58 (2002) 1987.
38 Silverstein M, Basseler G C & Morill C, Spectrometric Identification of Organic Compounds, Wiley, New York, 1981.
39 Barnes A J, Majid M A, Stuckey M A, Gregory P &. Stead C V, *Spectrochim Acta A,* 4 (1985) 629.
40 Mooney E F, *Spectrochim Acta A,* 20 (1964) 1021.
41 Bellamy L J, The Infra-red Spectra of Complex Molecules, Wiley, New York, 1975.
42 Sajan D, Binoy J, Pradeep B, Venkatakrishnan K, Kartha V B, Joe I H & Jayakumar V S, *Spectrochim Acta A,* 60 (2004) 173.

Appendix

Table A1 — Bond angles

Bond-angle (in °)	FluoroPA calculated	Bond-angle (in°)	ChloroPA calculated	ChloroPA experiment	Bond-angle (in°)	BromoPA calculated	BromoPA Experiment
C2-C1-C9	116.88	C3-C2-C10	117.2150	116.7	C3-C2-C10	117.1211	116.6
C2-C1-C11	120.81	C3-C2-C12	122.3254	122.4	C3-C2-C12	122.8993	122.6
C9-C1-C11	122.29	C10-C2-C12	120.4596	120.8	C10-C2-C12	119.9796	120.8
C1-C2-C3	123.32	Cl1-C3-C2	119.9892	119.7	Br1-C3-C2	120.4547	120.1
C1-C2-F18	118.21	Cl1-C3-C4	118.0048	117.8	Br1-C3-C4	117.542	117.2
C3-C2-F18	118.45	C2-C3-C4	122.0059	122.5	C2-C3-C4	122.0033	122.6
C2-C3-H4	119.50	C3-C4-H5	119.6481	120.4	C3-C4-H5	119.9072	120.5
C2-C3-C5	118.51	C3-C4-C6	119.4421	119.2	C3-C4-C6	119.4793	118.9
H4-C3-C5	121.98	H5-C4-C6	120.9097	120.4	H5-C4-C6	120.6135	120.5
C3-C5-H6	119.64	C4-C6-H7	119.5798	120.1	C4-C6-H7	119.5575	119.8
C3-C5-C7	120.01	C4-C6-C8	119.9112	120.1	C4-C6-C8	119.8894	120.4
H6-C5-C7	120.34	H7-C6-C8	120.5091	120.1	H7-C6-C8	120.5532	120.5
C5-C7-H8	120.18	C6-C8-H9	120.3277	120.0	C6-C8-H9	120.3445	120.2
C5-C7-C9	119.93	C6-C8-C10	119.7366	121.7	C6-C8-C10	119.7267	119.7
H8-C7-C9	119.88	H9-C8-C10	119.9358	120.0	H9-C8-C10	119.9288	120.2
C1-C9-C7	121.32	C2-C10-C8	121.6890	121.7	C2-C10-C8	121.7801	121.7
C1-C9-H10	118.89	C2-C10-H11	118.6649	119.1	C2-C10-H11	118.5992	119.1
C7-C9-H10	119.78	C8-C10-H11	119.6458	119.1	C8-C10-H11	119.6202	119.1
C1-C11-H12	110.51	C2-C12-H13	110.1177	108.4	C2-C12-H13	111.8229	108.5
C1-C11-H13	111.45	C2-C12-H14	111.7514	108.4	C2-C12-H14	110.0459	108.5
C1-C11-C14	113.96	C2-C12-C15	114.0458	115.5	C2-C12-C16	113.9969	115.2
H12-C11-H13	106.13	H13-C12-H14	106.2160	107.5	H13-C12-H14	106.2363	107.5
H12-C11-C14	107.12	H13-C12-C15	106.5489	108.4	H13-C12-C16	107.8909	108.5
H13-C11-C14	107.24	H14-C12-C15	107.7369	108.4	H14-C12-C16	106.4220	108.5
C11-C14-O15	126.78	C12-C15-O16	126.7216	123.5	C16-O15-H18	107.1440	115.0
C11-C14-O16	110.39	C12-C15-O17	110.4343	113.2	C12-C16-O15	110.4555	112.8
O15-C14-O16	122.81	O16-C15-O17	122.8273	123.3	C12-C16-O17	126.6835	123.9
C14-O16-H17	107.16	C15-O17-H18	107.1459	109.5	O15-C16-O17	122.8399	123.3

Table A2 — Dihedrals

Dihedral-angle (in°)	FluoroPA calculated	Dihedral-angle (in°)	ChloroPA Cal.	ChloroPA Expt.	Dihedral-angle (in°)	BromoPA Cal.	BromoPA Expt.
C9-C1-C2-F18	–179.6	C10-C2-C3-Cl1	–179.9	–179.2	C10-C2-C3-Br1	–179.9	178.8
C2-C1-C11-H12	–160.1	C10-C2-C3-C4	–0.03	-0.2	C10-C2-C3-C4	–0.01	–0.2
C2-C1-C11-H13	–42.3	C3-C2-C12-H13	–160.7	-	C3-C2-C12-H13	41.9	-
C2-C1-C11-C14	79.1	C3-C2-C12-H14	–42.9	-	C3-C2-C12-H14	159.7	-
C9-C1-C11-H12	20.0	C3-C2-C12-C15	79.5	68.3	C3-C2-C12-C16	–80.7	–68.9
C9-C1-C11-H13	137.7	C10-C2-C12-H13	19.1	-	C10-C2-C12-H13	–138.1	-
C9-C1-C11-C14	–100.6	C10-C2-C12-H14	136.9	-	C10-C2-C12-H14	–20.3	-
C2-C3-C5-H6	179.8	C10-C2-C12-C15	–100.5	–114.0	C10-C2-C12-C16	99.1	114.0
H4-C3-C5-C7	–179.9	C3-C4-C6-H7	179.9	108.4	C3-C4-C6-H7	–179.9	-
C3-C5-C7-H8	–179.9	H5-C4-C6-C8	179.9	-	H5-C4-C6-C8	–179.9	-
C3-C5-C7-C9	0.05	C4-C6-C8-H9	–179.9	-	C4-C6-C8-H9	–179.9	-
H6-C5-C7-H8	0.03	C4-C6-C8-C10	0.007	0.4	C4-C6-C8-C10	0.04	0.2
H6-C5-C7-C9	–179.9	H7-C6-C8-C10	179.9	-	H7-C6-C8-C10	–179.9	-
C5-C7-C9-H10	179.9	C6-C8-C10-H11	179.9	-	C6-C8-C10-H11	–179.8	-
H8-C7-C9-C1	–179.9	H9-C8-C10-C2	–179.8	-	H9-C8-C10-C2	179.8	-
H8-C7-C9-H10	–0.05	H9-C8-C10-H11	–0.07	-	H9-C8-C10-H11	0.14	-
C1-C11-C14-O15	5.09	C2-C12-C15-O16	11.2	15.7	C2-C12-C16-O15	169.1	166.1
C1-C11-C14-O16	–175.5	C2-C12-C15-O17	–170.1	–166.3	C2-C12-C16-O17	–12.4	–15.8
H12-C11-C14-O15	–117.4	H13-C12-C15-O16	–110.4	-	H13-C12-C16-O15	44.3	-
H12-C11-C14-O16	61.8	H13-C12-C15-O17	68.1	-	H13-C12-C16-O17	–137.2	-
H13-C11-C14-O15	128.9	H14-C12-C15-O16	135.9	-	H14-C12-C16-O15	–69.3	-
H13-C11-C14-O16	–51.7	H14-C12-C15-O17	–45.5	-	H14-C12-C16-O17	109.0	-